


 Cite this: *RSC Adv.*, 2022, **12**, 4501

Aluminium alkyl complexes supported by imino-phosphanamide ligand as precursors for catalytic guanylation reactions of carbodiimides†

 Himadri Karmakar, ^a Srinivas Anga, ^b Tarun K. Panda ^{*a} and Vadapalli Chandrasekhar ^{*bc}

Herein, we report the synthesis, characterisation, and application of three aluminium alkyl complexes, $[K^2\text{-}\{N\text{H}^R\text{P}(\text{Ph})\text{NDipp}\}\text{AlMe}_2]$ ($R = \text{Dipp}$ (**2a**), Mes (**2b**); tBu (**2c**), Dipp = 2,6-diisopropylphenyl, Mes = mesityl, and tBu = *tert*-butyl), supported by unsymmetrical imino-phosphanamide $[\text{N}\text{H}^R\text{P}(\text{Ph})\text{NDipp}]^-$ [$R = \text{Dipp}$ (**1a**), Mes (**1b**), tBu (**1c**)] ligands as molecular precursors for the catalytic synthesis of guanidines using carbodiimides and primary amines. All the imino-phosphanamide ligands **1a**, **1b** and **1c** were prepared in good yield from the corresponding N-heterocyclic imine (NHI) with phenylchloro-2,6-diisopropylphenylphosphanamine, $\text{PhP}(\text{Cl})\text{NH}\text{Dipp}$. The aluminium alkyl complexes **2a**, **2b** and **2c** were obtained in good yield upon completion of the reaction between trimethyl aluminium and the protic ligands **1a**, **1b** and **1c** in a 1 : 1 molar ratio in toluene *via* the elimination of methane, respectively. The molecular structures of the protic ligands **1b** and **1c** and the aluminium complexes **2a**, **2b** and **2c** were established *via* single-crystal X-ray diffraction analysis. Complexes **2a**, **2b** and **2c** were tested as pre-catalysts for the hydroamination/guanylation reaction of carbodiimides with aryl amines to afford guanidines at ambient temperature. All the aluminium complexes exhibited a high conversion with 1.5 mol% catalyst loading and broad substrate scope with a wide functional group tolerance during the guanylation reaction. We also proposed the most plausible mechanism, involving the formation of catalytically active three-coordinate Al species as the active pre-catalyst.

Received 13th January 2022

Accepted 17th January 2022

DOI: 10.1039/d2ra00242f

rsc.li/rsc-advances

Introduction

Metal-catalysed C–N bond formation is an intense area of research. One of the convenient strategies to achieve the C–N bond is the catalytic guanylation reaction.¹ This reaction is a hydroamination reaction, where the N–H bond of an amine adds across carbodiimide, which produces guanidine derivatives.² The metal-catalysed guanylation reaction is a 100% atom economy reaction and a straightforward method to prepare nitrogen-rich compounds.³ Guanidine derivatives are important due to their multipurpose usage in organic synthesis,⁴ coordination chemistry,⁵ pharmaceuticals,⁶ and the agrochemical industry. They are also important structural motifs of many

biologically and pharmaceutically active molecules. They can serve as building blocks in various pharmaceutical and natural products.⁷ Due to their low nucleophilicity, it is difficult for arylamines to participate in guanylation reactions with unactivated carbodiimides in the absence of a catalyst.⁸ In 2003, Richeson *et al.* reported the catalytic guanylation reaction between primary arylamines and unactivated carbodiimides for the first time using a titaniumimido complex as a catalyst at elevated temperatures.⁹ Further, the guanylation reaction of primary arylamines and carbodiimides has been investigated using transition-,¹⁰ rare-earth-,¹¹ and main group metal complexes.¹² Recently, we reported various titanium(IV) metal complexes and zinc(II) metal complex as precursors for the catalytic guanylation reaction of carbodiimides.¹³

Recent trends in synthetic chemistry demonstrate the increasing use of synthetic methods in multicomponent reactions and catalysis using earth-abundant metals. Multicomponent reactions emphasize the progress of reactions using fewer (compared to conventional reactions) steps, while the choice of earth-abundant metals is driven by their non-toxicity and economy. Therefore, aluminium, as the most abundant metal on earth and due to its non-toxic nature, has been used in complexes as a preeminent catalyst in several important multicomponent reactions. In 2009, the commercially available

^aDepartment of Chemistry, Indian Institute of Technology Hyderabad, Kandi, Sangareddy 502285, Telangana, India. E-mail: tpanda@iith.ac.in; Fax: +91 40 2301 6032; Tel: +91 40 2301 6036

^bTata Institute of Fundamental Research Hyderabad, Gopanpally, 500107, Hyderabad, India. E-mail: vc@tifrh.res.in

^cDepartment of Chemistry, IIT Kanpur, Kanpur 208016, India. E-mail: vc@iitk.ac.in

† Electronic supplementary information (ESI) available: Text giving experimental details for the catalytic reactions, ^1H , $^{13}\text{C}\{^1\text{H}\}$ and spectra of guanidines/guanylation products **3a**–**3v**, ligands **1b**, **1c** and aluminium metal complexes **2a**, **2b**, **2c**. CCDC 2124039–2124043. For ESI and crystallographic data in CIF or other electronic format see DOI: 10.1039/d2ra00242f



AlMe₃ was utilised as a catalyst for the guanylation reaction by Zhang and co-workers.¹⁴ Bergman's group and Zhou's group also used aluminium alkyl complexes as catalysts for guanylation reactions.¹⁵ Recently, Mandal *et al.* reported the use of a cyclic (alkyl) amino carbene complex of AlMe₃ as a catalyst for the guanylation reaction.¹⁶

There have been numerous studies on nitrogen-based electron rich ligands such as amidinate,^{17,18} guanidinate,^{18,19} iminophosphonamide,²⁰ and boraamidinate⁸⁻²¹ ligands. Accordingly, some of these ligands have already found wide applications in the formation of a range of metal complexes including the stabilisation of unusual oxidation states of main-group elements.¹⁸ Among them, the amidinate and guanidinate ligands have received significant attention by many research groups.¹⁷⁻¹⁹

Monoanionic N-heterocyclic imines such as imidazolin-2-iminato ligands are often described by two limiting resonance structures, thus indicating that the ability of the imidazolium ring to stabilise a positive charge leads to highly basic ligands²² with strong electron-donating capacity toward early transition metals.²³ Imidazolin-2-iminato ligands were successfully introduced in main group metals, transition metals, lanthanides, and more recently, actinide metals by Tamm and co-workers to achieve very short M-N bonds.²⁴ Our group and others²⁵ have already established that monoanionic imidazolin-2-iminato ligands are efficient systems for the preparation of catalytically active transition metal and rare earth metal complexes.²⁶

Recently, the exceptional electron-donating ability and fine-tuning of the steric properties of imidazolin-2-iminato ligands were utilised to stabilise main group metal ions. The isolation of a carbene-stabilised phosphorus mononitride,²⁷ monomeric phosphinyl radical,²⁸ singlet phosphononitrene,²⁹ its protonated derivative³⁰ and metal complexes was reported by Bertrand *et al.*³¹ The further utilisation of this ligand to stabilise several group 13- and group 16-metal ions was demonstrated by Inoue³²⁻³⁶ and Rivard.^{37,38} However, aluminium alkyl complexes with the imidazoline-2-iminato ligand were only recently studied by the research groups of Inoue,^{35,36} Masuda³⁹ and Eisen.⁴⁰

Recently, we developed an N-heterocyclic imine-based imino-phosphonamide ligand-supported yttrium complex $[\text{NHI}^R\text{P}(\text{Ph})\text{N}-\text{Dipp}]\text{Y}\{\text{NSiMe}_3\}_2$ (iPr, Me), where the ligand upon metalation is bonded with the yttrium ion in a monoanionic fashion similar to that of amidinate ligands.⁴¹ The two donor nitrogen atoms attached to the phosphorus atom are completely different and it is interesting to note that this system is amenable to stereoelectronic modulation through substitution at the phosphorus and nitrogen centers.⁴² Currently, we were interested in the interaction of the unsymmetrical imino-phosphonamide ligands with p-block elements such as aluminium and the exploration of the complexes formed in the catalytic guanylation reaction. Accordingly, herein, we report the synthesis and characterisation of imino-phosphonamine ligands $[\text{NHI}^R\text{P}(\text{Ph})\text{NHDipp}]$ [R = Dipp (**1a**), Mes (**1b**), *t*Bu (**1c**)] and the corresponding aluminium alkyl complexes $[\text{NHI}^R\text{P}(\text{Ph})\text{NDipp}]\text{AlMe}_2$ (R = Dipp (**2a**), Mes (**2b**); *t*Bu (**2c**)), respectively, together with the catalytic applications of the latter

towards the guanylation of primary arylamines with unactivated carbodiimides.

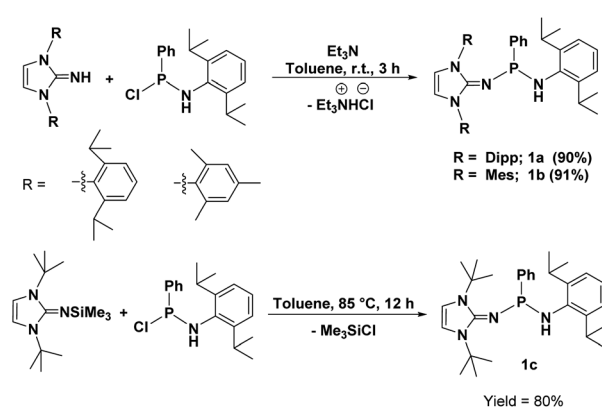
Results and discussion

Ligand synthesis

The protic ligands **1a** and **1b** were synthesised according to the protocol involving the reaction of imidazolin-2-imine $[\text{Im}^R\text{NH}]$ (R = Dipp and Mes) with $\text{PhP}(\text{Cl})\text{NH}(\text{Dipp})$ (Dipp = 2,6-diisopropylphenyl) (1 : 1 equiv.) in the presence of triethylamine (1.5 equiv.) at room temperature, as previously reported by us.⁴¹ The ligand **1c** was obtained in 80% yield by the reaction between 1,3-di-*tert*-butyl-2-(trimethylsilylimino)imidazoline and $\text{PhP}(\text{Cl})\text{NH}(\text{Dipp})$ in a 1 : 1 molar ratio at 85 °C in toluene *via* the elimination of trimethylsilyl chloride (Scheme 1). All three ligands, **1a**, **1b** and **1c**, were characterised using ¹H, ¹³C{¹H} and ³¹P{¹H} NMR spectroscopy, and elemental analysis.

The multinuclear NMR spectra of ligand **1a** and its molecular structure in the solid-state were previously reported by us.²² The solid-state structures of **1b** and **1c** were established by single-crystal X-ray diffraction analysis. In the ¹H NMR spectrum, the signal for the amine NH hydrogen atom appears at $\delta_{\text{H}} = 3.98$ ppm as a broad singlet for **1b**, whereas the signal for a similar NH hydrogen atom of **1c** appears at $\delta_{\text{H}} = 4.59$ ppm as a doublet due to its coupling with the phosphorus atom [$^2J_{\text{HP}}$ of 3 Hz (**1c**)]. The two olefinic protons of the imidazole ring display a singlet resonance at $\delta_{\text{H}} = 5.61$ ppm (**1b**) and 6.07 ppm (**1c**). Three singlet peaks at $\delta_{\text{H}} = 2.26$, 2.14 and 1.96 ppm appear in the ¹H NMR spectrum of **1b** due to the three methyl groups of the mesityl unit and a sharp singlet at $\delta_{\text{H}} = 1.46$ ppm in the ¹H NMR spectrum of **1c** appears due to the 18 methyl protons of its two *tert*-butyl groups. Further, a septet signal centered at $\delta_{\text{H}} = 3.45$ ppm (**1b**) and 3.52 ppm (**1c**) and two doublets at $\delta_{\text{H}} = 1.13$ and 1.06 ppm (**1b**) and 1.27 and 1.18 ppm (**1c**) were observed due to the protons of the isopropyl groups attached to the Dipp moiety. In the ³¹P{¹H} NMR spectra, compounds **1b** and **1c** exhibit a sharp singlet at $\delta_{\text{P}} = 73.13$ ppm (**1b**) and 78.2 ppm (**1c**).

Compound **1b** crystallises in the triclinic *P*1 space group, whereas **1c** crystallises in the monoclinic *P*2₁/n space group. The molecular structures of **1b** and **1c** in the solid-state are given in



Scheme 1 Synthesis of the protic ligands **1a**, **1b**, and **1c**.



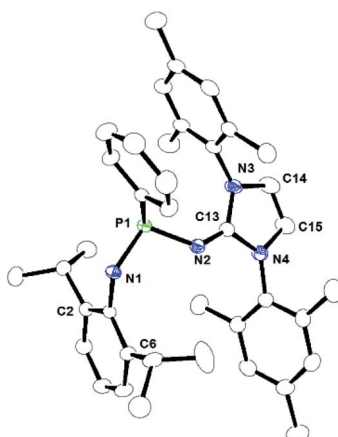


Fig. 1 ORTEP drawing of the molecular structure of **1b**, where ellipsoids are drawn to encompass 30% probability, while hydrogen atoms were omitted for clarity. Selected bond lengths [Å] and bond angles [°]: P1–N1 1.7346(11), P1–N2 1.6844(12), P1–C24 1.8390(13), N2–C13 1.2944(18), N3–C13 1.3853(18), N4–C13 1.3815(18), N1–P1–N2 102.91(6), N1–P1–C24 93.10(6), N2–P1–C24 104.11(6), N2–C13–N3 130.67(13), N2–C13–N4 125.01(13), N3–C13–N4 104.30(12). CCDC no. 2124041.†

Fig. 1 and 2, respectively. The P–N1 and P–N2 bond distances of 1.7346(11) Å and 1.6844(12) Å (**1b**) and 1.729(2) Å and 1.652(2) Å (**1c**) are similar. Similar P–N bond distances were also observed in compound **1a** (1.670(1) Å and 1.741(1) Å).²² The N1–P1–N2 bond angles in **1b** (102.91(6)°) and **1c** (102.63(12)°) are much wider than that in **1a** (93.79°) due to the less steric crowding in compounds **1b** and **1c**.

Aluminium bisalkyl complexes

Trimethyl aluminium (AlMe_3) was reacted with one equivalent of protic ligands **1a**, **1b**, and **1c** to afford, in good yield (Scheme 2), the corresponding aluminium-bisalkyl complexes [κ^2 – $\{\text{NHI}^R\text{P}(\text{Ph})\text{NDipp}\}\text{AlMe}_2$] ($R = \text{Dipp}$ (**2a**), Mes (**2b**), $t\text{Bu}$ (**2c**)), respectively. These compounds are highly soluble in benzene, toluene, and THF, but partially soluble in *n*-hexane and diethyl

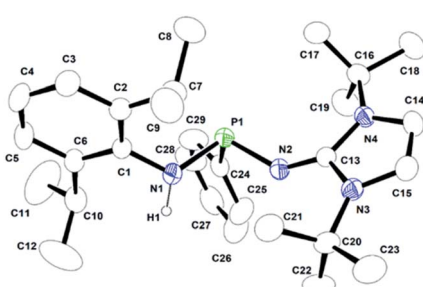
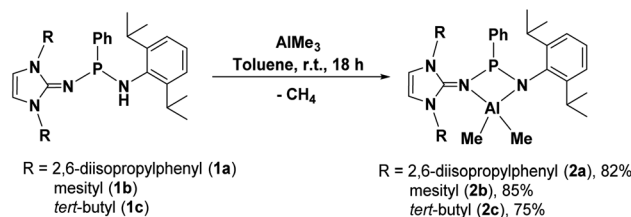


Fig. 2 ORTEP drawing of the molecular structure of **1c**, where ellipsoids are drawn to encompass 30% probability, while hydrogen atoms were omitted for clarity. Selected bond lengths [Å] and bond angles [°]: P1–N1 1.729(2), P1–N2 1.652(2), P1–C24 1.848(3), N2–C13 1.292(3), N3–C13 1.386(4), N4–C13 1.394(3), N1–P1–N2 102.63(12), N1–P1–C24 98.45(13), N2–P1–C24 99.86(13), N2–C13–N3 123.4(2), N2–C13–N4 131.6(3), N3–C13–N4 104.6(2). CCDC no. 2124043.†



Scheme 2 Synthesis of Al-alkyl complexes **2a** and **2b**.

ether. **2a**, **2b**, and **2c** were characterised *via* ^1H , $^{13}\text{C}\{^1\text{H}\}$ and $^{31}\text{P}\{^1\text{H}\}$ NMR spectral data and elemental analysis. Further, the solid-state structures of **2a**, **2b**, and **2c** were established by single-crystal X-ray crystallography.

Well-resolved NMR spectra measured in C_6D_6 were obtained for **2a**, **2b**, and **2c**. In their ^1H NMR spectra, the absence of resonance signals at $\delta_{\text{H}} = 3.73$, 3.98, and 4.59 ppm confirmed the deprotonation of the NH proton of ligands **1a**, **1b**, and **1c**, respectively. The six protons corresponding to the AlMe_2 unit appeared as a sharp singlet at $\delta_{\text{H}} = -0.73$ ppm for **2a**, -0.57 and -0.60 ppm for **2b** and -0.19 ppm for **2c** in the ^1H NMR spectra. Additionally, signals corresponding to the isopropyl groups of two Dipp moieties and methyl groups of two mesityl moieties were also observed for **2a** and **2b**, respectively. For **2c**, a sharp singlet at $\delta_{\text{H}} = 0.99$ ppm for the protons from the *tert*-butyl group was observed. In the $^{31}\text{P}\{^1\text{H}\}$ NMR spectra, **2a**, **2b** and **2c** exhibit singlets at $\delta_{\text{P}} = 134.64$ ppm, 130.60 ppm and 158.64 ppm, respectively, which are significantly shifted downfield compared to that of the corresponding ligands, which are $\delta_{\text{P}} = 71.79$ ppm (**1a**), 73.13 ppm (**1b**) and 78.26 ppm (**1c**).

The solid-state structures of complexes **2a**, **2b** and **2c** were determined by single-crystal X-ray diffraction analysis, which confirmed the attachment of the unsymmetrical imino-phosphanamide $[\text{NHI}^R\text{P}(\text{Ph})\text{NDipp}]$ ligand to the aluminium ion. Complexes **2a** and **2c** crystallise in the monoclinic space group $P2_1/n$ and $P2_1/c$, respectively, and complex **2b** crystallises in the triclinic space group $\bar{P}\bar{1}$. The crystallographic details and refinement parameters are given in Table TS1 in the ESI.† The molecular structures of **2a**, **2b** and **2c** in their solid state are shown in Fig. 3, 4 and 5 respectively.

2a, **2b**, and **2c** are monomeric and their coordination polyhedrons are formed by the chelation of two nitrogen atoms from the monoanionic imino-phosphanamide $[\text{NHI}^R\text{P}(\text{Ph})\text{NDipp}]^-$ moiety. The aluminium ions are asymmetrically attached to the ligand backbone, as indicated by the Al1–N1 bond distances of **2a**, **2b**, and **2c** [1.8642(19) Å, 1.8679(11) Å and 1.8979(12) Å, respectively] and the Al1–N2 bond distances of **2a**, **2b** and **2c** [2.0022(18) Å, 1.9903(11) Å and 1.9401(12) Å, respectively]. The anionic amido nitrogen atoms are better electron donors towards the Al(III) cation than the imino-phosphanamide nitrogen atoms. In all the complexes, the central aluminium ion is four-fold coordinated due to the coordination of two nitrogens from the imino-phosphanamide ligand and two methyl groups are attached to the metal ion in each case. The geometry around the aluminium ion in each



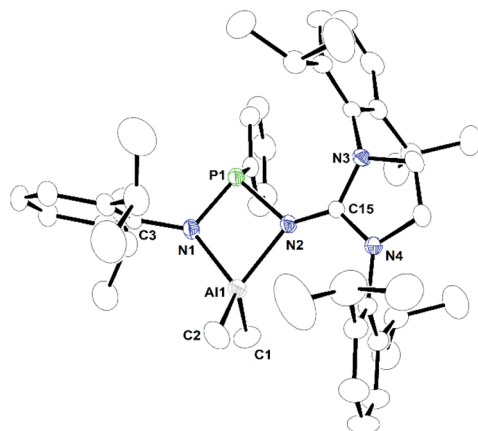


Fig. 3 ORTEP drawing of the molecular structure of **2a**, where ellipsoids are drawn to encompass 30% probability, while hydrogen atoms were omitted for clarity. Selected bond lengths [\AA] and bond angles [$^\circ$]: Al1–N1 1.8642(19), Al1–N2 2.0022(18), Al1–C1 1.974(3), Al1–C2 1.952(3), N2–C15 1.316(2), N3–C15 1.380(3), N4–C15 1.372(2), N1–P1–N2 88.67(8), N1–Al1–N2 76.96(7), N1–Al1–C1 115.89(11), N1–Al1–C2 114.02(13), C1–Al1–C2 107.79(17), N2–Al1–C1 117.37(13), N2–Al1–C2 122.14(13), N2–C15–N3 130.04(18), N2–C15–N4 124.93(18), N3–C15–N4 105.02(16). CCDC no. 2124040.†

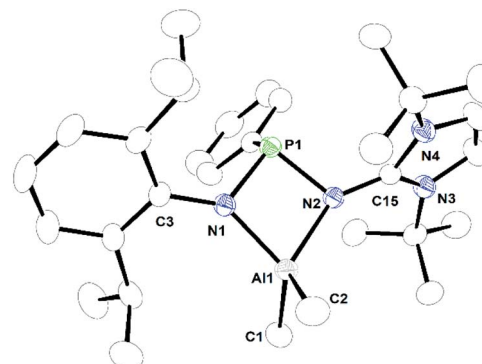


Fig. 5 ORTEP drawing of the molecular structure of **2c**, where ellipsoids are drawn to encompass 30% probability, while hydrogen atoms were omitted for clarity. Selected bond lengths [\AA] and bond angles [$^\circ$]: Al1–N1 1.8979(12), Al1–N2 1.9401(12), Al1–C1 1.987(2), Al1–C2 1.968(2), N2–C15 1.3479(18), N3–C15 1.3722(18), N4–C15 1.372(2), N1–P1–N2 89.26(6), N1–Al1–N2 78.36(5), N1–Al1–C1 120.36(8), N1–Al1–C2 115.83(8), C1–Al1–C2 108.41(10), N2–Al1–C1 115.77(7), N2–Al1–C2 115.77(8), N2–C15–N3 125.48(13), N2–C15–N4 128.37(13), N3–C15–N4 106.06(12). CCDC no. 2124039.†

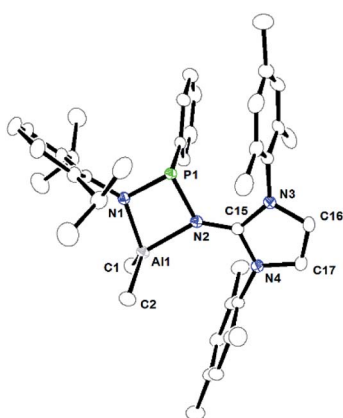


Fig. 4 ORTEP drawing of the molecular structure of **2b**, where ellipsoids are drawn to encompass 30% probability, while hydrogen atoms were omitted for clarity. Selected bond lengths [\AA] and bond angles [$^\circ$]: Al1–N1 1.8679(11), Al1–N2 1.9903(11), Al1–C1 1.9672(17), Al1–C2 1.9698(17), N2–C15 1.3177(17), N3–C15 1.3714(16), N4–C15 1.3688(17), N1–P1–N2 88.41(5), N1–Al1–N2 77.16(5), N1–Al1–C1 114.64(7), N1–Al1–C2 114.21(7), C1–Al1–C2 112.97(8), N2–Al1–C1 117.61(6), N2–Al1–C2 115.69(7), N2–C15–N3 130.10(12), N2–C15–N4 125.01(11), N3–C15–N4 104.89(11). CCDC no. 2124042.†

complex can best be described as distorted tetrahedral. In each complex, one four-membered metallacycle Al1–N1–P1–N2 is formed, suggesting molecular strain.

Catalytic study

At the outset of our study, the efficiency of **2a**, **2b**, and **2c** towards the catalytic hydroamination/guanylation of various aryl amines with carbodiimides was studied. The catalytic experiments were performed using equimolar amounts of

carbodiimides and primary amines. The benchmark guanylation reaction of 2-bromoaniline with *N,N'*-diisopropylcarbodiimide (DIC) was chosen to check the efficiency of **2a** and **2b** as precatalysts. In the case of amine addition, due to the fact that $-\text{NH}_2$ is a diprotic nucleophile, isomerisation of the initial product occurs, leading to guanidine derivatives (**3a**–**3v**) as the major products. In each case, the corresponding guanidine products were isolated and purified by washing with *n*-pentane and the results are given in Table 1. As a control experiment, a blank reaction was carried out at 60 °C for 20 h in the presence of only diisopropyl carbodiimide (DIC) and 2-bromoaniline, which showed that no guanidine product was formed (Table 1, entry 1). However, in the presence of 0.5 mol% **2a** as a precatalyst, 71% of substituted guanidine **3a** was achieved as the product at room temperature within a reaction time of 6 h (Table 1, entry 2). Under the same reaction conditions, **2b** yielded 72% of product **3a** (Table 1, entry 3). When the catalyst loading was increased to 1.0 mol%, and finally to 1.5 mol% for **2a**, a substantial increase in the product yield up to 89% was observed within 2 h at room temperature (Table 1, entries 4 and 6). However, under the same conditions, complex **2b** did not show much improvement in the product yield (Table 1, entries 5 and 7). The use of precatalyst **2c** gave 83% of product **3a** under similar conditions (Table 1, entry 8). To optimise the solvent effect, the catalytic reactions were carried out in different solvents such as *n*-hexane and THF as well as in neat conditions at room temperature. However, we did not observe any major effect of solvent on the catalytic reaction.

After the preliminary evaluation of the catalysts for the hydroamination of DIC, we concluded that complex **2a** is more efficient than **2b** at room temperature and in toluene solvent. With room temperature and toluene as the solvent being the optimal reaction settings for the hydroamination of carbodiimides, we set out to examine the scope of various substituted aryl amine and carbodiimide substrates in the presence of



Table 1 Optimisation study of the guanylation reaction between 2-bromoaniline and DIC^{a,b,c}

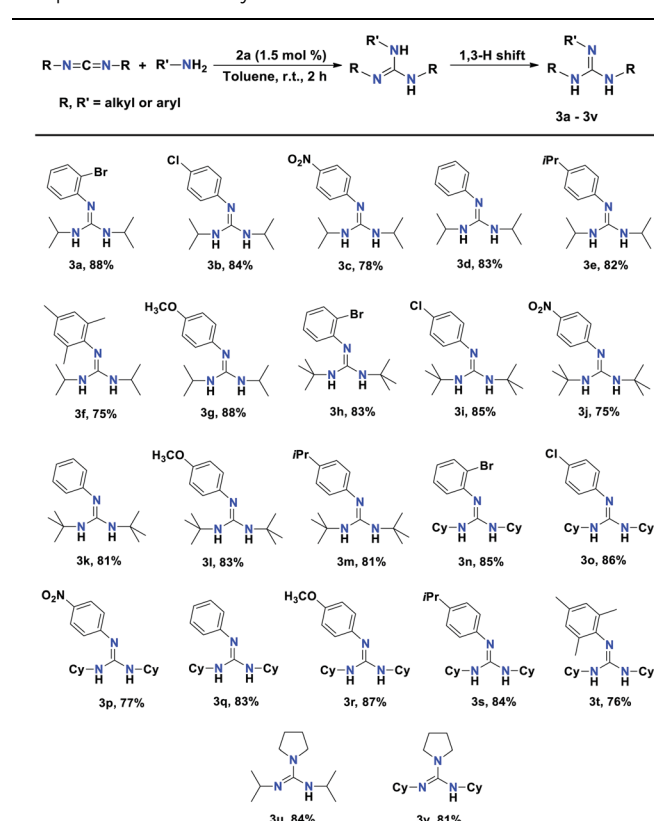
Entry	Catalyst	Mol%	Solvent	Time (h)	Yield (%)	Reaction scheme:	
						Al-catalyst x mol%	solvent, r.t., time
1			Toluene	20	0		
2	2a	0.5	Toluene	6	71		
3	2b	0.5	Toluene	6	72		
4	2a	1	Toluene	2	88		
5	2b	1	Toluene	2	85		
6	2a	1.5	Toluene	2	89		
7	2b	1.5	Toluene	2	86		
8	2c	1.5	Toluene	2	83		
9	2a	1.5	Hexane	2	82		
10	2b	1.5	Hexane	2	81		
11	2a	1.5	THF	2	85		
12	2b	1.5	THF	2	86		
13	2a	1.5	Neat	2	88		
14	2b	1.5	Neat	2	87		

^a Reaction conditions: Al complex **2a** (1.5 mol%), toluene solvent, room temperature, 2 h (optimised reaction time). ^b Compounds were isolated and purified by washing with *n*-pentane. ^c Yields were calculated from isolated pure products.

1.5 mol% of aluminium complex **2a** as the precatalyst. The results of the catalytic hydroamination reactions are displayed in Table 2. All the products **3a–3v** were fully characterised with the help of NMR spectroscopy and the yields were calculated from the isolated yields.

Substituted aryl amines containing electron-withdrawing groups, such as bromo, chloro, and nitro anilines reacted with DIC, affording very good yields (78–88%) of the desired guanidines within 2 h at room temperature (**3a–3c**), respectively. The unsubstituted aniline afforded 83% yield under the optimal conditions (Table 2, **3d**). The aryl amines with electron-donating groups such as 4-isopropyl aniline, 2,4,6-trimethylaniline, and 4-methoxy aniline exhibited excellent conversion, affording the corresponding guanidines within 2 h at room temperature (Table 2, **3e–3g**), respectively.

The substrate scope was further expanded by using *N,N*-di-*tert*-butylcarbodiimide and *N,N*-dicyclohexylcarbodiimide (DCC) with various arylamines in the presence of aluminium catalyst **2a**. The reaction of aniline with *N,N*-di-*tert*-butylcarbodiimide afforded 81% yield of the corresponding guanidine product. Anilines with electron-releasing groups and deactivated anilines with electron-withdrawing groups reacted smoothly with two carbodiimides, *N,N*-di-*tert*-butylcarbodiimides and DCC, resulting in the corresponding guanidine products in excellent yields (Table 2, entries **3h–3t**). This indicates the high efficiency of the aluminium complex **2a**. Pyrrolidine, which is a secondary amine, also reacted smoothly with DIC under the optimised condition to afford *N,N*-

Table 2 Hydroamination of various arylamines to carbodiimides using complex **2a** as the catalyst^{a,b,c}

^a Reaction conditions: Al complex **2a** (1.5 mol%), toluene solvent, room temperature, 2 h (optimised reaction time). ^b Compounds were isolated and purified by washing with *n*-pentane. ^c Yields were calculated from isolated pure products.

diisopropylpyrrolidine-1-carboximidamide (**3u**) and *N,N*-dicyclohexylpyrrolidine-1-carboximidamide (**3v**) in 84% and 81% yield (Table 2, **3u** and **3v**), respectively.

To explore the conversion of amine to guanidine and the highest possible efficiency of catalyst **2a**, the insertion of aniline into DIC was monitored using ¹H NMR spectroscopy, showing the progress of the reaction as a function of DIC consumption followed by the formation of guanidine. The insertion of aniline into DIC was monitored at 10 minute intervals using ¹H NMR spectroscopy, showing the formation of the guanidine product as a function of DIC consumption with time. The yield of the guanidine product was plotted against time, as shown in Fig. 6. It was observed that the formation of the guanidine product was very fast in the initial 20 min, and then it gradually slowed down after 2 h to attain saturation.

Most plausible mechanism

To explore the most plausible mechanism for the catalytic addition of N–H to carbodiimides, we performed some controlled reactions. Given that our ligand fragment contains a P-atom, it was easy for us to monitor the catalytic reaction through ³¹P{¹H} NMR measurement. The stoichiometric



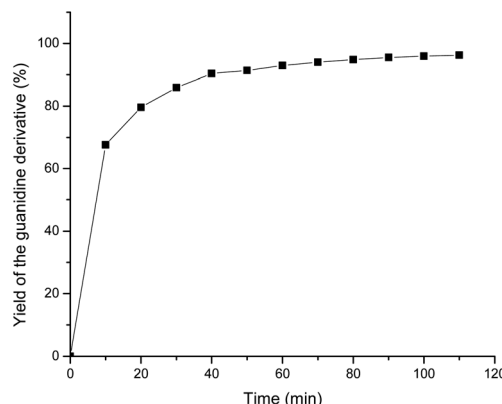


Fig. 6 Plot of the yield of the guanidine derivative (%) vs. time (min) as monitored by ^1H -NMR spectroscopy for the reaction between 2-bromoaniline and DIC at room temperature.

reaction of catalyst **2a** with DIC was carried out in benzene-d₆ and the ^1H and $^{31}\text{P}\{^1\text{H}\}$ NMR spectra of the reaction mixture suggested no reaction even at 70 °C. The Al-complex **2a** was treated with primary arylamine *p*-anisidine in a 1 : 2 molar ratio at room temperature. In the product, we detected one sharp singlet at δ_{P} 71.79 ppm in the $^{31}\text{P}\{^1\text{H}\}$ NMR spectrum, and in the ^1H NMR spectrum a singlet peak at $\delta_{\text{H}} = 3.73$ ppm also appeared, which is ascribed to the NH proton of free ligand **1a** (Fig. FS54 and FS55 in the ESI,† respectively). Analogously, the reaction of **2a** with a secondary amine such as piperidine in a 1 : 2 molar ratio at 70 °C gave one sharp singlet at δ_{P} 71.79 ppm in the $^{31}\text{P}\{^1\text{H}\}$ NMR spectrum and $\delta_{\text{H}} = 3.73$ ppm in the ^1H NMR spectrum, confirming the formation of free ligand **1a** (Fig. FS56 and FS57 in the ESI,† respectively). Thus, we easily observed the dissociation of the ligand moiety from the metal ion.

Based on these experiments, the catalytic cycle is proposed (Scheme 3) to proceed *via* amine exchange with the supporting

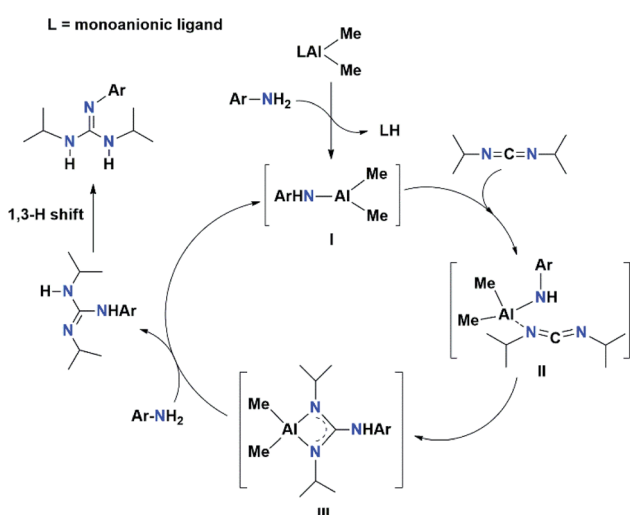
ligand to form a catalytically active three-coordinate Al species, which can subsequently add to carbodiimides to form Al guanidinate species. The catalytically active species can then be regenerated by another amine exchange reaction with free aniline. A similar mechanism was also reported by other research groups.¹⁵ The first step in this mechanism involves the rapid protonolysis of the ligand fragment of the aluminium catalyst **2a** by the N–H moiety of ArNH_2 , with the displacement of free ligand **1a**, producing an active three-coordinate Al species (I). In the next step, the carbodiimide molecule is bonded to Al species I to form Al guanidinate species III. Further, species III undergoes an amine exchange reaction with the free aniline in the final step to regenerate active species I.

Conclusions

In summary, we synthesised and characterised three unsymmetrical imino-phosphanamide-supported aluminium alkyl complexes and established their solid-state structures. The aluminium complex **2a** acted as an efficient catalyst for the guanylation reaction of arylamines and carbodiimides at room temperature. The three different carbodiimides underwent guanylation reactions to provide near-quantitative yields of the corresponding guanidines at ambient temperature within short reaction times. The most plausible mechanism for the catalytic addition of the N–H bond of arylamine to carbodiimides was also described. The key features of this protocol include the high catalytic efficiency of the aluminium complex **2a** with a wider substrate scope of carbodiimides and aryl amines at ambient temperature.

General experimental procedures

All manipulations involving air- and moisture-sensitive compounds were carried out under argon, using the standard Schlenk technique or argon-filled M. Braun glove box. Hydrocarbon solvents (*n*-hexane, toluene, and benzene) were distilled under a nitrogen atmosphere from LiAlH_4 and stored inside the glove box. THF was dried and deoxygenated by distillation over sodium benzophenone under argon and then distilled and dried over CaH_2 before being stored in the glove box. ^1H NMR (300 MHz), $^{31}\text{P}\{^1\text{H}\}$ (121.5 MHz) and $^{13}\text{C}\{^1\text{H}\}$ (75 MHz) spectra were recorded on a Nano Bay 300 MHz spectrometer. Elemental analyses were performed on a BRUKER EURO EA at the Indian Institute of Technology Hyderabad. Imidazolin-2-imines [$\text{Im}^{\text{R}}\text{NH}$] (R = Dipp, Mes) or their silylated derivative [$\text{Im}^{\text{R}}\text{NSiMe}_3$] (R = *t*Bu) prepared according to the published procedure.¹⁷ The protic ligand **1a** was synthesised according to our previously reported method.²² Trimethylaluminium, all amines, diisopropyl-carbodiimide, *N,N*-di-*tert*-butylcarbodiimide, and *N,N*-dicyclohexylcarbodiimide were purchased from Sigma Aldrich. Amines were distilled over CaH_2 before use. NMR spectroscopy solvent C_6D_6 was purchased from Sigma Aldrich, India and dried over Na/K , distilled, and stored in a glove box.



Scheme 3 Most plausible mechanism for guanylation reaction between carbodiimide and aryl amines mediated by aluminium complex **2a** as a precatalyst.



Preparation of $[\text{Im}^{\text{Mes}}\text{NP}(\text{Ph})\text{NH}(\text{Dipp})]$ (1b)

In a flame-dried 50 ml Schlenk flask, 500 mg (1.56 mmol) 1,3-bis(mesyl)imidazolin-2-imine and triethylamine (0.22 ml, 1.56 mmol) were dissolved in 20 ml toluene. Then $\text{PhP}(\text{Cl})\text{NH}(\text{Dipp})$ ($\text{Dipp} = 2,6\text{-diisopropylphenyl}$) (500 mg, 1.56 mmol) in 20 ml toluene was added dropwise to the mixture. The reaction mixture was allowed to stir for 3 h at room temperature. Subsequently, the reaction mixture was filtered to obtain a clear solution and the solvent was evaporated from the filtrate. A white solid powder was obtained, which was further washed with hexane. The compound was recrystallised from a toluene/hexane mixture at room temperature. White crystals were obtained after 2 days.

1b: yield: 858 mg, 91%. ^1H NMR (300 MHz, C_6D_6 , 298 K): δ_{H} 7.53 (t, $J = 6$ Hz, 2H, Ar-H), 7.13–6.98 (m, 6H, Ar-H), 6.77 (s, 2H, Ar-H), 6.64 (s, 2H, Ar-H), 5.61 (s, 2H, NCH), 3.98 (bs, 1H, NH), 3.49–3.40 (m, 2H, $\text{CH}(\text{CH}_3)_2$), 2.26 (s, 6H, CH_3), 2.14 (s, 6H, CH_3), 1.96 (s, 6H, CH_3), 1.13 (d, $J = 9$ Hz, 6H, CH_3), 1.06 (d, $J = 6$ Hz, 6H, CH_3) ppm. $^{13}\text{C}\{^1\text{H}\}$ NMR (75 MHz, C_6D_6 , 298 K): δ_{C} 150.38, 150.13, 145.70, 145.37, 140.97, 140.85, 138.33, 137.80, 137.10, 134.15, 129.93, 129.62, 129.22, 129.05, 123.31, 122.71, 113.79, 28.43, 28.35, 24.12, 24.09, 23.98, 21.12, 18.55, 18.49, 18.00 ppm. $^{31}\text{P}\{^1\text{H}\}$ NMR (121.5 MHz, C_6D_6 , 298 K): δ_{P} 73.13 ppm. Elemental analysis for $\text{C}_{39}\text{H}_{47}\text{N}_4\text{P}$ (602.7). Calcd for C 77.71, H 7.86, N 9.29; found C 77.63, H 7.58, N 9.03.

Preparation of $[\text{Im}^{t\text{Bu}}\text{NP}(\text{Ph})\text{NH}(\text{Dipp})]$ (1c)

In a flame-dried 50 ml Schlenk flask, 332 mg (1.24 mmol) 1,3-di-*tert*-butyl-2-(trimethylsilylimino)imidazoline was added and dissolved in 25 ml toluene. Then $\text{PhP}(\text{Cl})\text{NH}(\text{Dipp})$ ($\text{Dipp} = 2,6\text{-diisopropylphenyl}$) (396.16 mg, 1.24 mmol) in 20 ml toluene was added dropwise to the mixture. The reaction mixture was allowed to stir for 12 h at 85 °C. Subsequently, the reaction mixture was filtered to obtain a clear solution and the solvent was evaporated from the filtrate. A white solid powder was obtained, which was further washed with hexane. The compound was recrystallised from a toluene/hexane mixture at room temperature. White crystals were obtained after 2 days.

1c: yield: 475 mg, 80%. ^1H NMR (300 MHz, C_6D_6 , 298 K): δ_{H} 7.90 (t, $J = 6$ Hz, 2H, Ar-H), 7.26 (t, $J = 6$ Hz, 2H, Ar-H), 7.18–7.07 (m, 4H, Ar-H), 6.07 (s, 2H, NCH), 4.59 (d, $J = 3$ Hz, 1H, NH), 3.57–3.48 (m, 2H, $\text{CH}(\text{CH}_3)_2$), 1.46 (s, 18H, CH_3), 1.27 (s, 6H, CH_3), 1.18 (s, 6H, CH_3) ppm. $^{13}\text{C}\{^1\text{H}\}$ NMR (75 MHz, C_6D_6 , 298 K): δ_{C} 149.35, 149.13, 147.11, 146.67, 141.21, 140.47, 130.09, 129.80, 123.81, 122.50, 108.78, 55.75, 29.61, 28.69, 24.45, 24.24 ppm. $^{31}\text{P}\{^1\text{H}\}$ NMR (121.5 MHz, C_6D_6 , 298 K): δ_{P} 78.26 ppm. Elemental analysis for $\text{C}_{31}\text{H}_{48}\text{N}_4\text{P}$ (506.7). Calcd for C 73.48, H 9.35, N 11.06; found C 73.31, H 9.21, N 10.93.

Preparation of $[\kappa^2\text{-}\{\text{Im}^{\text{R}}\text{NP}(\text{Ph})\text{NDipp}\}\text{AlMe}_2]$ ($\text{R} = \text{Dipp}$ (2a), Mes (2b), *t*Bu (2c))

In a flame-dried 25 ml Schlenk flask, ligand **1a** (200 mg, 0.29 mmol) or **1b** (179 mg, 29 mmol) or **1c** (134 mg, 0.29 mmol) was added and dissolved in 15 ml toluene. Then trimethylaluminium solution (2 M) in toluene (0.15 ml, 0.29 mmol) was added

to it under ice-cold conditions and stirred at room temperature for 18 h. Next, the solvent was evaporated, and the residue was washed with hexane. The crude product was recrystallised from a toluene/hexane mixture at room temperature.

2a: yield: 177.3 mg, 82%. ^1H NMR (300 MHz, C_6D_6 , 298 K): δ_{H} 7.34 (t, $J = 6$ Hz, 3H, Ar-H), 7.21–7.13 (m, 3H, Ar-H), 7.07–7.02 (m, 5H, Ar-H), 6.93 (d, $J = 9$ Hz, 3H, Ar-H), 5.89 (s, 2H, NCH), 3.28–3.19 (m, 4H, $\text{CH}(\text{CH}_3)_2$), 2.81–2.72 (m, 2H, $\text{CH}(\text{CH}_3)_2$), 1.64 (d, $J = 6$ Hz, 6H, CH_3), 1.04 (d, $J = 6$ Hz, 18H, CH_3), 0.94 (d, $J = 9$ Hz, 12H, CH_3), –0.73 (s, 6H, Al-CH₃) ppm. $^{13}\text{C}\{^1\text{H}\}$ NMR (75 MHz, C_6D_6 , 298 K): δ_{C} 150.57, 149.76, 149.16, 149.00, 147.92, 146.79, 141.32, 141.11, 133.00, 131.40, 129.88, 129.54, 124.93, 124.80, 122.84, 118.39, 29.61, 29.43, 26.71, 26.35, 25.93, 22.47, 22.13, –3.50, –5.01 ppm. $^{31}\text{P}\{^1\text{H}\}$ NMR (121.5 MHz, C_6D_6 , 298 K): δ_{P} 134.64 ppm. Elemental analysis for $\text{C}_{47}\text{H}_{64}\text{AlN}_4\text{P}$ (743.0) (2a). Calcd for C 75.98, H 8.68, N 7.54; found C 75.63, H 8.39, N 7.32.

2b: yield: 162 mg, 85%. ^1H NMR (300 MHz, C_6D_6 , 298 K): δ_{H} 7.45 (s, 2H, Ar-H), 7.07 (s, 6H, Ar-H), 6.83 (s, 2H, Ar-H), 6.61 (s, 2H, Ar-H), 5.33 (s, 2H, NCH), 4.07 (bs, 1H, $\text{CH}(\text{CH}_3)_2$), 3.65 (bs, 1H, $\text{CH}(\text{CH}_3)_2$), 2.32 (s, 6H, CH_3), 2.12 (s, 6H, CH_3), 1.66 (s, 6H, CH_3), 1.54 (bs, 6H, CH_3), 1.17 (bs, 3H, CH_3), 0.40 (bs, 3H, CH_3), –0.57 (s, 3H, Al-CH₃), –0.60 (s, 3H, Al-CH₃) ppm. $^{13}\text{C}\{^1\text{H}\}$ NMR (75 MHz, C_6D_6 , 298 K): δ_{C} 151.06, 150.27, 145.73, 145.58, 142.15, 141.96, 140.37, 138.46, 138.39, 137.08, 131.62, 131.60, 131.40, 131.04, 129.85, 129.56, 129.34, 123.08, 123.04, 115.82, 21.11, 18.47, 18.41, 17.87, –4.36, –4.67 ppm. $^{31}\text{P}\{^1\text{H}\}$ NMR (121.5 MHz, C_6D_6 , 298 K): δ_{P} 130.60 ppm. Elemental analysis for $\text{C}_{41}\text{H}_{52}\text{AlN}_4\text{P}$ (658.8) (2b). Calcd for C 74.74, H 7.96, N 8.50; found C 74.58, H 7.83, N 8.42.

2c: yield: 112 mg, 75%. ^1H NMR (300 MHz, C_6D_6 , 298 K): δ_{H} 8.11 (q, $J = 7$ Hz, 2H, Ar-H), 7.16–7.10 (m, 6H, Ar-H), 5.82 (s, 2H, NCH), 4.20–4.06 (m, 1H, $\text{CH}(\text{CH}_3)_2$), 3.98–3.84 (m, 1H, $\text{CH}(\text{CH}_3)_2$), 1.58 (d, $J = 6$ Hz, 3H, CH_3), 1.47 (d, $J = 6$ Hz, 3H, CH_3), 1.19 (d, $J = 6$ Hz, 3H, CH_3), 0.99 (s, 18H, CH_3), 0.83 (d, $J = 6$ Hz, 3H, CH_3), –0.19 (s, 6H, Al-CH₃) ppm. $^{13}\text{C}\{^1\text{H}\}$ NMR (75 MHz, C_6D_6 , 298 K): δ_{C} 150.80, 150.64, 139.38, 139.24, 137.80, 134.53, 134.32, 131.16, 124.71, 123.87, 115.21, 61.83, 31.97, 31.04, 29.06, 25.30, 25.02, 23.06, 14.37, –4.13 ppm. $^{31}\text{P}\{^1\text{H}\}$ NMR (121.5 MHz, C_6D_6 , 298 K): δ_{P} 158.46 ppm. Elemental analysis for $\text{C}_{31}\text{H}_{48}\text{AlN}_4\text{P}$ (534.6) (2c). Calcd for C 69.63, H 9.05, N 10.48; found C 69.54, H 8.87, N 10.29.

General procedure for catalytic guanylation reaction

In a 25 ml Schlenk flask, aromatic primary amine (1 mmol) and carbodiimide (1 mmol) were added and 2 ml toluene was added to form a homogeneous mixture. Then complex **2a** (1.5 mol%) was added to the reaction mixture as a precatalyst. The mixture was allowed to stir at room temperature for 2 h. Then the solvent was evaporated, and the residue was extracted by ether. After evaporation of the ether, the final product was obtained by washing with *n*-pentane. The products were characterised by ^1H and $^{13}\text{C}\{^1\text{H}\}$ NMR spectroscopy and details are given in the ESL.†

Conflicts of interest

There are no conflicts to declare.



Acknowledgements

H. K. thanks CSIR India for his Ph.D. fellowships (09/1001(0038)/2018-EMR-I). Instrumental support was provided by the Indian Institute of Technology Hyderabad and TIFR Hyderabad.

Notes and references

- (a) C. Alonso-Moreno, A. Antiñolo, F. Carrillo-Hermosilla and A. Otero, *Chem. Soc. Rev.*, 2014, **43**, 3406; (b) S. Raouf moghaddam, *Org. Biomol. Chem.*, 2014, **12**, 7179; (c) W.-X. Zhang and Z. Hou, *Org. Biomol. Chem.*, 2008, **6**, 1720; (d) W.-X. Zhang, L. Xu and Z. Xi, *Chem. Commun.*, 2015, **51**, 254.
- F. Montilla, D. del Río, A. Pastor and A. Galindo, *Organometallics*, 2006, **25**, 4996.
- (a) S. Zhou, S. Wang, G. Yang, Q. Li, L. Zhang, Z. Yao, Z. Zhou and H.-B. Song, *Organometallics*, 2007, **26**, 3755; (b) H. Shen, H.-S. Chan and Z. Xie, *Organometallics*, 2006, **25**, 5515; (c) M. R. Crimmin, A. G. M. Barrett, M. S. Hill, P. B. Hitchcock and P. A. Procopiou, *Organometallics*, 2008, **27**, 497.
- (a) X. Fu and C.-H. Tan, *Chem. Commun.*, 2011, **47**, 8210; (b) J. C. McManus, T. Genski, J. S. Carey and R. J. K. Taylor, *Synlett*, 2003, **3**, 369; (c) T. Ishikawa and T. Isobe, *Chem.-Eur. J.*, 2002, **8**, 553; (d) B. Kovačević and Z. B. Maksić, *Org. Lett.*, 2001, **3**, 1523.
- (a) P. M. Coles, *Dalton Trans.*, 2006, **8**, 985; (b) F. T. Edelmann, *Chem. Soc. Rev.*, 2012, **41**, 7657.
- (a) D. Castagnolo, S. Schenone and M. Botta, *Chem. Rev.*, 2011, **111**, 5247; (b) R. G. S. Berlinck, A. E. Trindade-Silva and M. F. C. Santos, *Nat. Prod. Rep.*, 2012, **29**, 1382; (c) R. G. S. Berlinck, A. C. B. Burtoloso, A. E. Trindade-Silva, S. Romminger, R. P. Morais, K. Bandeira and C. M. Mizuno, *Nat. Prod. Rep.*, 2010, **27**, 1871.
- (a) E. J. Corey, B. Czakó and L. Kürti, *Molecules and medicine*, Wiley, Hoboken, NJ, 1st edn, 2007; (b) C. Anselmi, A. Ettorre, M. Andreassi, M. Centini, P. Neri and A. Di Stefano, *Biochem. Pharmacol.*, 2002, **63**, 437; (c) G. Byk, J. Soto, C. Mattler, M. Frederic and D. Scherman, *Biotechnol. Bioeng.*, 1998, **61**, 81.
- T. P. Hopkins, J. M. Dener and A. M. Boldi, *J. Comb. Chem.*, 2002, **4**, 167.
- T.-G. Ong, G. P. A. Yap and D. S. Richeson, *J. Am. Chem. Soc.*, 2003, **125**, 8100.
- (a) F. Montilla, A. Pastor and A. Galindo, *J. Organomet. Chem.*, 2004, **689**, 993; (b) D. Li, J. Guang, W.-X. Zhang, Y. Wang and Z. Xi, *Org. Biomol. Chem.*, 2010, **8**, 1816; (c) H. Shen and Z. Xie, *J. Organomet. Chem.*, 2009, **694**, 1652.
- (a) X. Zhu, Z. Du, F. Xu and Q. Shen, *J. Org. Chem.*, 2009, **74**, 6347; (b) Q. Li, S. Wang, S. Zhou, G. Yang, X. Zhu and Y. Liu, *J. Org. Chem.*, 2007, **72**, 6763; (c) Z. Du, W. Li, X. Zhu, F. Xu and Q. Shen, *J. Org. Chem.*, 2008, **73**, 8966; (d) W.-X. Zhang, M. Nishiura and Z. Hou, *Chem.-Eur. J.*, 2007, **13**, 4037; (e) Y. Wu, S. Wang, L. Zhang, G. Yang, X. Zhu, C. Liu, C. Yin and J. Rong, *J. Organomet. Chem.*, 2009, **362**, 2814.
- (a) C. Alonso-Moreno, F. Carrillo-Hermosilla, A. Garcés, A. Otero, I. López-Solera, A. M. Rodríguez and A. Antiñolo, *Organometallics*, 2010, **29**, 2789; (b) J. R. Lachs, A. G. M. Barrett, M. R. Crimmin, G. Kociok-Köhnn, M. S. Hill, M. F. Mahon and P. A. Procopiou, *Eur. J. Inorg. Chem.*, 2008, **26**, 4173; (c) T.-G. Ong, J. S. O'Brien, I. Korobkov and D. S. Richeson, *Organometallics*, 2006, **25**, 4728; (d) L. Xu, Y.-C. Wang, W. Ma, W.-X. Zhang and Z. Xi, *J. Org. Chem.*, 2014, **79**, 12004.
- (a) S. Das, J. Bhattacharjee and T. K. Panda, *Dalton Trans.*, 2019, **48**, 7227; (b) J. Bhattacharjee, S. Das, R. K. Kottalankaa and T. K. Panda, *Dalton Trans.*, 2016, **45**, 17824; (c) J. Bhattacharjee, M. Sachdeva, I. Banerjee and T. K. Panda, *J. Chem. Sci.*, 2016, **128**, 875.
- W.-X. Zhang, D. Li, Z. Wang and Z. Xi, *Organometallics*, 2009, **28**, 882.
- (a) J. Koller and R. G. Bergman, *Organometallics*, 2010, **29**, 5946; (b) Y. Wei, S. Wang, S. Zhou, Z. Feng, L. Guo, X. Zhu, X. Mu and F. Yao, *Organometallics*, 2015, **34**, 1882.
- P. K. Vardhanapu, V. Bheemireddy, M. Bhunia, G. Vijaykumar and S. K. Mandal, *Organometallics*, 2018, **37**, 2602.
- (a) P. C. Junk and M. L. Cole, *Chem. Commun.*, 2007, 1579–1590; (b) F. T. Edelmann, *Chem. Soc. Rev.*, 2009, **38**, 2253–2268; (c) F. T. Edelmann, *Chem. Soc. Rev.*, 2012, **41**, 7657–7672; (d) J. A. R. Schmidt and J. J. Arnold, *J. Chem. Soc., Dalton Trans.*, 2002, 3454–3461; (e) C. A. Nijhuis, E. Jellema, T. J. J. Sciarone, A. Meetsma, P. H. M. Budzelaar and B. Hessen, *Eur. J. Inorg. Chem.*, 2005, 2089–2099; (f) D. A. Kissounko, M. V. Zabalov, G. P. Brusova and D. A. Lemenovskii, *Russ. Chem. Rev.*, 2006, **75**, 351–374.
- (a) P. J. Bailey and S. Pace, *Coord. Chem. Rev.*, 2001, **214**, 91–141; (b) A. A. Trifonov, *Coord. Chem. Rev.*, 2010, **254**, 1327–1347; (c) S. T. Barry, *Coord. Chem. Rev.*, 2013, **257**, 3192–3201.
- (a) R. Vollmerhaus, R. Tomaszewski, P. Shao, N. J. Taylor, K. J. Wiacek, S. P. Lewis, A. Al-Humydi and S. Collins, *Organometallics*, 2005, **24**, 494–507; (b) B. Nekoueishahraki, H. W. Roesky, G. Schwab, D. Stern and D. Stalke, *Inorg. Chem.*, 2009, **48**, 9174–9179; (c) N. Nebra, C. Lescot, P. Dauban, S. Mallet-Ladeira, B. Martin-Vaca and D. Bourissou, *Eur. J. Org. Chem.*, 2013, **2013**, 984–990; (d) A. Stasch, *Angew. Chem., Int. Ed.*, 2014, **53**, 10200–10203; (e) B. Prashanth and S. Singh, *Dalton Trans.*, 2014, **43**, 16880–16888; (f) A. L. Hawley and A. Stasch, *Eur. J. Inorg. Chem.*, 2015, **2015**, 258–270; (g) K. A. Rufanov, N. K. Pruss and J. Sundermeyer, *Dalton Trans.*, 2016, **45**, 1525–1538; (h) S. Wingerter, M. Pfeiffer, A. Murso, C. Lustig, T. Stey, V. Chandrasekhar and D. Stalke, *J. Am. Chem. Soc.*, 2001, **123**, 1381–1388; (i) A. Stasch, *Chem.-Eur. J.*, 2012, **12**, 15105–15112; (j) T. J. Feuerstein, B. Goswami, P. Rauthe, R. Koppe, S. Lebedkin, M. M. Kappes and P. W. Roesky, *Chem. Sci.*, 2019, **10**, 4742–4749.
- (a) C. Fedorchuk, M. Copsey and T. Chivers, *Coord. Chem. Rev.*, 2007, **251**, 897–924; (b) A. M. Corrente, M. Andrea and T. Chivers, *Inorg. Chem.*, 2010, **49**, 2457–2463; (c) S. Harder and D. Naglav, *Eur. J. Inorg. Chem.*, 2010, **18**,



- 2836–2840; (d) S. Harder, *Dalton Trans.*, 2010, **39**, 6677–6681; (e) S. Harder, B. Freitag, P. Stegner, J. Pahl and D. Naglav, *Z. Anorg. Allg. Chem.*, 2015, **641**, 2129–2134; (f) T. Chivers, D. J. Eisler, C. Fedorchuk, G. Schatte, H. M. Tuononen and R. T. Boere, *Inorg. Chem.*, 2006, **45**, 2119–2131; (g) T. Chivers, D. J. Eisler, C. Fedorchuk, G. Schatte, H. M. Tuononen and R. T. Boere, *Chem. Commun.*, 2005, 3930–3932.
- 21 (a) S. P. Green, C. Jones and A. Stasch, *Science*, 2007, **318**, 1754–1757; (b) S. J. Bonyhady, D. Collis, G. Frenking, N. Holzmann, C. Jones and A. Stasch, *Nat. Chem.*, 2010, **2**, 865–869; (c) S. S. Sen, A. Jana, H. W. Roesky and C. Schulzke, *Angew. Chem., Int. Ed.*, 2009, **48**, 8536–8538; (d) S. Nagendran, S. S. Sen, H. W. Roesky, D. Koley, H. Grubmüller, A. Pal and R. Herbst-Irmer, *Organometallics*, 2008, **27**, 5459–5463; (e) C. Jones, *Coord. Chem. Rev.*, 2010, **254**, 1273–1289; (f) S. P. Green, C. Jones, P. C. Junk, K.-A. Lippert and A. Stasch, *Chem. Commun.*, 2006, 3978–3980; (g) M. K. Bisai, V. S. V. S. N. Swamy, T. Das, K. Vanka, R. G. Gonnade and S. S. Sen, *Inorg. Chem.*, 2019, **58**, 10536–10542; (h) V. S. V. S. N. Swamy, K. V. Raj, K. Vanka, S. S. Sen and H. W. Roesky, *Chem. Commun.*, 2019, **55**, 3536–3539; (i) S. Pahar, S. Karak, M. Pait, K. V. Raj, K. Vanka and S. S. Sen, *Organometallics*, 2018, **37**, 1206–1213.
- 22 M. Tamm, D. Petrovic, S. Randoll, S. Beer, T. Bannenberg, P. G. Jones and J. Grunenberg, *Org. Biomol. Chem.*, 2007, **5**, 523–530.
- 23 (a) M. Tamm, S. Randoll, T. Bannenberg and E. Herdtweck, *Chem. Commun.*, 2004, 876–877; (b) M. Tamm, S. Beer and E. Herdtweck, *Z. Naturforsch., B: J. Chem. Sci.*, 2004, **59**, 1497–1504; (c) M. Tamm, S. Randoll, E. Herdtweck, N. Kleigrewe, G. Kehr, G. Erker and B. Rieger, *Dalton Trans.*, 2006, 459–467; (d) S. Beer, C. G. Hrib, P. G. Jones, K. Brandhorst, J. Grunenberg and M. Tamm, *Angew. Chem., Int. Ed.*, 2007, **46**, 8890–8894; (e) S. Beer, K. Brandhorst, J. Grunenberg, C. G. Hrib, P. G. Jones and M. Tamm, *Org. Lett.*, 2008, **10**, 981–984; (f) S. H. Stelzig, M. Tamm and R. M. Waymouth, *J. Polym. Sci., Part A: Polym. Chem.*, 2008, **46**, 6064–6070; (g) S. Beer, K. Brandhorst, C. G. Hrib, X. Wu, B. Haberlag, J. Grunenberg, P. G. Jones and M. Tamm, *Organometallics*, 2009, **28**, 1534–1545.
- 24 (a) A. G. Trambitas, T. K. Panda and M. Tamm, *Z. Anorg. Allg. Chem.*, 2010, **636**, 2156–2171; (b) X. Wu and M. Tamm, *Coord. Chem. Rev.*, 2014, **260**, 116–138; (c) T. K. Panda, S. Randoll, C. G. Hrib, P. G. Jones, T. Bannenberg and M. Tamm, *Chem. Commun.*, 2007, 5007–5009; (d) S. Beer, K. Brandhorst, J. Grunenberg, C. G. Hrib, P. G. Jones and M. Tamm, *Org. Lett.*, 2008, **10**, 981–984; (e) D. Petrovic, L. M. R. Hill, P. G. Jones, W. B. Tolman and M. Tamm, *Dalton Trans.*, 2008, 887–894; (f) D. Petrovic, C. G. Hrib, S. Randoll, P. G. Jones and M. Tamm, *Organometallics*, 2008, **27**, 778–783; (g) S. Beer, K. Brandhorst, C. G. Hrib, X. Wu, B. Haberlag, J. Grunenberg, P. G. Jones and M. Tamm, *Organometallics*, 2009, **28**, 1534–1545; (h) T. K. Panda, A. G. Trambitas, T. Bannenberg, C. G. Hrib, S. Randoll, P. G. Jones and M. Tamm, *Inorg. Chem.*, 2009, **48**, 5462–5472; (i) A. G. Trambitas, T. K. Panda, J. Jenter, P. W. Roesky, C. Daniliuc, C. G. Hrib, P. G. Jones and M. Tamm, *Inorg. Chem.*, 2010, **49**, 2435–2446; (j) T. K. Panda, C. G. Hrib, P. G. Jones and M. Tamm, *J. Organomet. Chem.*, 2010, **695**, 2768–2773; (k) M. Tamm, A. G. Trambitas, C. G. Hrib and P. G. Jones, *Terra Rare*, 2010, **7**, 1–4; (l) A. G. Trambitas, D. Melcher, L. Hartenstein, P. W. Roesky, C. Daniliuc, P. G. Jones and M. Tamm, *Inorg. Chem.*, 2012, **51**, 6753–6761; (m) I. Karmel, M. Botoshansky, M. Tamm and M. S. Eisen, *Inorg. Chem.*, 2014, **53**, 694–696; (n) S. Das, J. Bhattacharjee and T. K. Panda, *New J. Chem.*, 2019, **43**, 16812.
- 25 N. Kuhn, M. Göhner, M. Grathwohl, J. Wiethoff, G. Frenking and Y. Chen, *Z. Anorg. Allg. Chem.*, 2003, **629**, 793–802.
- 26 T. K. Panda, C. G. Hrib, P. G. Jones, J. Jenter, P. W. Roesky and M. Tamm, *Eur. J. Inorg. Chem.*, 2008, **2008**, 4270.
- 27 R. Kinjo, B. Donnadieu and G. Bertrand, *Angew. Chem., Int. Ed.*, 2010, **49**, 5930–5933.
- 28 O. Back, B. Donnadieu, M. von Hopffgarten, S. Klein, R. Tonner, G. Frenking and G. Bertrand, *Chem. Sci.*, 2011, **2**, 858–861.
- 29 F. Dielmann, O. Back, M. Henry-Ellinger, P. Jerabek, G. Frenking and G. Bertrand, *Science*, 2012, **337**, 1526–1528.
- 30 F. Dielmann, C. E. Moore, A. L. Rheingold and G. Bertrand, *J. Am. Chem. Soc.*, 2013, **135**, 14071–14073.
- 31 F. Dielmann, D. M. Andrade, G. Frenking and G. Bertrand, *J. Am. Chem. Soc.*, 2014, **136**, 3800–3802.
- 32 T. Ochiai and S. Inoue, *Phosphorus, Sulfur Silicon Relat. Elem.*, 2016, **191**, 624–627.
- 33 T. Ochiai, D. Franz, X. Wu and S. Inoue, *Dalton Trans.*, 2015, **44**, 10952–10956.
- 34 D. Franz, T. Szilvasi, E. Irran and S. Inoue, *Nat. Commun.*, 2015, **6**, 10037–10042.
- 35 D. Franz, E. Irran and S. Inoue, *Dalton Trans.*, 2014, **43**, 4451–4461.
- 36 D. Franz and S. Inoue, *Chem.-Eur. J.*, 2014, **20**, 10645–10649.
- 37 M. W. Lui, N. R. Paisley, R. McDonald, M. J. Ferguson and E. Rivard, *Chem.-Eur. J.*, 2016, **22**, 2134–2145.
- 38 M. W. Lui, C. Merten, M. J. Ferguson, R. McDonald, Y. Xu and E. Rivard, *Inorg. Chem.*, 2015, **54**, 2040–2049.
- 39 A. D. K. Todd, W. L. McClellan and J. D. Masuda, *RSC Adv.*, 2016, **6**, 69270–69276.
- 40 H. Liu, M. Khononov, N. Fridman, M. Tamm and M. S. Eisen, *Inorg. Chem.*, 2019, **58**, 13426–13439.
- 41 (a) S. Anga, J. Acharya and V. Chandrasekhar, *J. Org. Chem.*, 2021, **86**, 2224; (b) S. Anga, H. Karmakar, T. K. Panda and V. Chandrasekhar, *J. Organomet. Chem.*, 2021, **954**–955, 122091.
- 42 (a) X. Wu and M. Tamm, *Coord. Chem. Rev.*, 2014, **260**, 116–138; (b) T. Ochiai, D. Franz and S. Inoue, *Chem. Soc. Rev.*, 2016, **45**, 6327–6344, see also references cited therein.

